Proposal to the ISOLDE and Neutron Time-of-Flight Committee

Penning-trap mass measurements of Zn and Cu isotopes relevant for the astrophysical rp-process

June 3, 2016

D. Atanasov[1], K. Blaum[1], S. George[1], F. Herfurth[2], A. Herlert[3], D. Lunney[4], Yu. A. Litvinov[2], A. Kankainen[5], V. Manea[6], M. Mougeot[4], D. Neidherr[2], C. Langer[7], M. Rosenbusch[8], L. Schweikhard[8], F. Wienholtz[8], R. N. Wolf[1], A. Welker[9], and K. Zuber[9]

[1]*Max-Planck-Institut für Kernphysik, Saupfercheckweg 1, 69117 Heidelberg, Germany*
[2]*GSI Helmholtzzentrum für Schwerionenforschung GmbH, 64291 Darmstadt, Germany*
[3]*FAIR GmbH, Darmstadt, Germany*
[4]*CSNSM-IN2P3-CNRS, Université Paris-Sud, 91406 Orsay, France*
[5]*University of Jyväskylä, FI-40014 Jyväskylä, Finland*
[6]*CERN, 1211 Geneva, Switzerland*
[7]*Goethe-Universität Frankfurt a. M., Frankfurt am Main, Germany*
[8]*Ernst-Moritz-Arndt-Universität, Institut für Physik, 17487 Greifswald, Germany*
[9]*Technische Universität Dresden, 01069 Dresden, Germany*

Spokespersons:
Dinko Atanasov [dinko.atanasov@cern.ch], Anu Kankainen [anu.kankainen@jyu.fi]
Contact person:
Dinko Atanasov [dinko.atanasov@cern.ch]

Abstract

We propose to measure the masses of the two neutron-deficient ^{58}Zn and ^{56}Cu isotopes. The masses are of great importance to understand how the rapid proton capture process (rp process) can proceed beyond the ^{56}Ni waiting point in type I X-ray bursts. The resonant proton-capture rates depend exponentially on the proton separation energies, and thus on the masses. It is crucial to be able to model the rp-process flow around the ^{56}Ni region more precisely as it influences the observed light curves as well as the burst ashes which contribute to the composition of the underlying neutron star crust. Presently, the proton-capture Q value of ^{56}Cu, 190(200) keV, is based on the systematic trends in the mass surface [1], while in the case of ^{58}Zn it was measured but has insufficient precision 2279(50) keV [2] to be used in modern type I X-ray burst models. In addition, the mass measurements of ^{56}Cu and ^{58}Zn provide data on the mass surface near the doubly magic ^{56}Ni and more precise Q_{EC} values for their beta decays.

Requested shifts: 12 shifts on a ZrO_2 felt target with laser ionization

1 Motivation

Type I X-ray bursts are among the frequent types of stellar explosions observed in the Galaxy. In terms of output energy in one single event these objects rank third after supernovae and classical novae [3]. The first X-ray burst was observed 40 years ago [4] and to date the number of observed X-ray bursts have increased to 106. A popular scenario identifies the X-ray binary systems to be consisting of a neutron star and a main-sequence companion star. Soon after the discovery, it was realized that the energy released during the bursts, lasting about 10-200 seconds, stems from a thermonuclear runaway occurring in degenerate conditions by accreting material on the neutron star's surface [5, 6]. High temperature and densities make a triple-alpha reaction possible, which is further followed by CNO cycle and eventually the temperature becomes high enough to break out from the hot CNO cycle and trigger a rapid nucleosynthesis [7] through the so-called rapid proton capture process (rp-process) [8, 9]. The rp-process is a sequence of proton captures and subsequent β^+-decays taking place along the proton drip line. The time scale for the thermal runaway ranges between 10-100 s and the amount of energy released can be directly observed as an X-ray outburst of typically 10^{39} ergs per second. Several X-ray space observatories have been commissioned in recent years, from which more and more new data on Type I X-ray bursts have become available [10]. For understanding the new observations and the contribution of type I X-ray bursts on the composition of the underlying neutron star crust, detailed nuclear reaction network calculations are needed. Of particular importance to the reaction-network calculations of the rp-process are the nuclear masses, of neutron-deficient nuclides found along its path [7].

Of special interest are the so-called waiting points in the rp-process, such as the doubly magic ^{56}Ni, that were shown to qualitatively explain the extended tails observed in the light curves of the X-ray burst [11]. A waiting point is a nucleus close to the proton drip line where the proton-capture Q values are low or even negative and β-decay half-lives are relatively long, thus hindering the reaction flow towards heavier elements. The net effect in the process is waiting for the slow beta-decay, which on the other hand delays the overall nuclear burning and extends the energy release of the burst. ^{56}Ni has a beta-decay half-life of 6.075(10) days, and it is one of the most interesting rp-process waiting points, determining whether the process can proceed beyond nickel or not. This will have a direct effect on the type I X-ray burst light curve as well as the ashes left after the bursts. Recently, the key resonant states in ^{58}Zn relevant for the ^{57}Cu(p,γ)^{58}Zn reaction were measured using the GRETINA gamma-detector array at NSCL, MSU [12]. The remaining uncertainties affecting the reaction flow beyond ^{56}Ni are related to the mass of ^{58}Zn as already shown by Forstner et al. [13]. Figure 1 and Fig. 2 presents the influence due to the mass uncertainty on the light curve of X-ray burst model and the associated reaction rates. Currently, the mass of ^{58}Zn is based on the measurements of the Q-value in a double charge-exchange reaction (^{58}Ni(π^+,π^-)^{58}Zn) performed 30 years ago [2]. The resulting value of the mass excess was found to be $-42.295(50)$ MeV. We propose measurements by using the state-of-the-art high-precision mass spectrometer ISOLTRAP, to improve the precision in the mass-excess value below 10 keV. Recently, the dependence of X-ray burst models on uncertainties from nuclear reaction rates, such as (p,γ) and (α,γ), have been studied by using fully self-consistent burst models. The latter

account for the feedbacks between changes in nuclear energy generation and changes in astrophysical conditions [14]. In these studies, the reaction rate for ^{57}Cu(p,γ)^{58}Zn was shown to have a high impact on the model calculations.
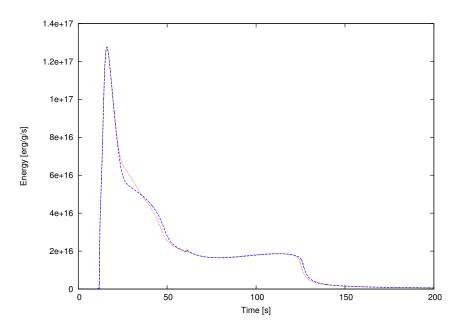

Figure 1: Calculated X-ray burst light curve using a one-zone self-consistent model (Schatz et al. [7]). The distinct difference between the two curves results solely from varying the Q-value of the ^{57}Cu(p,γ)^{58}Zn reaction up (red dotted) and down (blue dashed). The uncertainty in the reaction Q-value is dominated by the uncertainty of the mass of ^{58}Zn, which currently is $\sigma = 50$ keV. For our calculation we used a variation of 2σ up and down.

Another important case to study that can influence the reaction flow in the region around the nickel waiting point is ^{55}Ni(p,γ)^{56}Cu. The uncertainty in the Q-value for this reaction is mainly due to the mass of ^{56}Cu. Currently the nuclear mass tabulated in Atomic Mass Evaluation 2012 (AME12) [1] is only an extrapolation with an uncertainty of 200 keV. In a recent publication [15], the authors determined indirectly the nuclear mass by using local mass formulas such as the Improved Garvey-Kelson mass relation (ImGK) [16] and the Coulomb Displacement Energy mass relation (CDE) [17]. These approaches are very popular whenever the experimental mass data in the neutron-deficient region is missing. The study found a deviation of 500 keV to the extrapolations published in AME12. If a deviation of this magnitude is confirmed, it will significantly affect the proton-capture ^{55}Ni(p,γ)^{56}Cu and the photo-disintegration rates ^{56}Cu(γ,p)^{55}Ni during the rp-process, finally influencing the reaction flow at the ^{56}Ni waiting point. Furthermore, since the extrapolated proton-capture Q-value is rather low, the direct mass measurement of ^{56}Cu would also yield information on the proton drip line in this region.

The masses of ^{56}Cu and ^{58}Zn are also crucial for understanding the mass surface near the doubly-magic ^{56}Ni. Of these, ^{58}Zn represents a special case where spin-isospin symmetry in the pf shell [18, 19] and the isospin symmetry of analogous transitions can be studied. An

3

improvement in the Q_{EC} value of ^{58}Zn would result in more precise beta-decay strengths [20, 21] to be compared with the strengths from (^{3}He,t) charge-exchange reactions [22] for testing the isospin symmetry of analogous transitions. The beta-decay of ^{58}Zn has been recently studied with excellent statistics at GANIL, thus the mass measurement would be very timely.
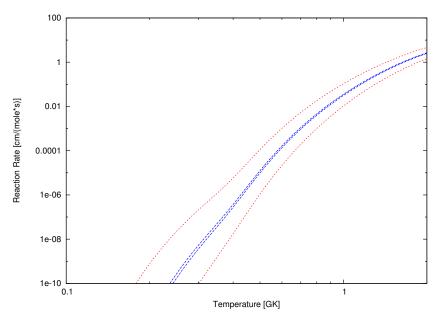

Figure 2: The ^{57}Cu(p,γ)^{58}Zn reaction rate using different Q-values for the reaction. The red dotted lines present the reaction rates when varying the Q-value by 100-keV up and down (or 2 sigma of its uncertainty). Especially at low temperatures the rates differ by more than 2 orders of magnitude. With the blue dashed lines are the same rates presented but only by using 5-keV uncertainty in the Q-value.

2 Experimental setup

The proposed measurements would be performed using the versatile mass spectrometer ISOLTRAP [23, 24]. Nowadays the setup comprises a linear, radio-frequency quadrupole cooler and buncher (RFQ), a multi-reflection time-of-flight mass spectrometer (MR-TOF MS) and two Penning traps (one frequently used separation and preparation of ion bunches and one used for precision mass spectrometery). A recent review of the current setup was published in [25]. The MR-TOF MS has become a device routinely used at ISOLTRAP either as a beam purifier [24] or beam analyzer [26]. Using this device one has the advantage to extend the mass measurement program at ISOLTRAP by performing mass measurements of very short-lived species not accessible via Penning trap [27–29].

To reach a high precision, the experiment requires an isobarically pure, low-emittance beam. We expect that the biggest isobaric contamination would be stable or long-lived Ni and/or Fe produced in the target. The required mass resolving power for both cases is about $3 \cdot 10^3$. The mass resolving power of HRS is fortunately sufficient to provide

such isobaric mass separation. Afterwards, the 50-keV continuous beam from ISOLDE is first injected in the RFQ for bunching and cooling via collisions with a helium buffer gas. Afterwards, the ions are transported as a bunch toward the MR-TOF MS for beam analysis. The MR-TOF MS routinely reaches resolving powers of about 10^5 after several 10 ms of flight time, which would be sufficient for further purification of the ion beam. As a next step the ions are injected in the first Penning trap for preparation purposes, such as cooling and cleaning. The ions are then send to the precision Penning trap for performing the actual high-precision mass measurements employing the so-called time-of-flight ion-cyclotron-resonance technique (TOF-ICR) [30].

3 Beam-time request

The table below presents the requested shifts of radioactive beam for the two isotopes of interest. The number of the needed shifts, required for setting-up the measurement cycle of ISOLTRAP, the MR-TOF MS and the identification in the precision Penning trap using the TOF-ICR technique are given separately (2 shifts for preparation per isotope). The information of the half-life was taken from [31, 32]. The yield information was collected from the ISOLDE Yield database [33]. Two target materials were listed to produce Zn and Cu isotopes - Nb foil and ZrO_2 felt. A higher production rate and faster release is achieved by the latter material. The production yield is possible only with RILIS laser ion source. In the case of ^{56}Cu yield information is not available and the value in the table is an estimation taking into account its half-life and the yield of ^{57}Cu ($3 \cdot 10^3$ ions/μC^{-1}) [33]. The number of the calculated shifts are based on the yield expectation of 10 ions/μC^{-1}.

Isotope	Half-life (ms)	Yield (ions/μC^{-1})	Target/ion source	Method	Shifts (8h)
^{58}Zn	86.7(24)	10	ZrO_2/RILIS	Penning trap and/or MR-TOF MS	2+4
^{56}Cu	93(6)	10^0 - 10^2	ZrO_2/RILIS	Penning trap and/or MR-TOF MS	2+4

Summary of requested shifts: 12 shifts of neutron-deficient ^{58}Zn and ^{56}Cu beams from ZrO_2 felt target material with RILIS ion source.

References

1. M. Wang *et al.*, *Chinese Phys. C* **36**, 1603 (2012).

2. K. K. Seth *et al.*, *Phys. Lett. B* **173**, 397 –399 (1986).

3. A. Parikh *et al.*, *Prog. Part. Nuc. Phys.* **69**, 225 –253 (2013).

4. J. Grindlay *et al.*, *Astrophys. J.* **205**, L127–L130 (May 1976).

5. P. C. Joss, *Nature* **270**, 310 (5635 Nov. 1977).

6. S. E. Woosley *et al.*, *Nature* **263**, 101 (1976).

7. H. Schatz *et al.*, *Nuc. Phys. A* **777**, 601 –622 (2006).

8. R. Wallace *et al.*, *Apys. J* **45**, 389–420 (Feb. 1981).

9. H. Schatz *et al.*, *Physics Reports* **294**, 167 –263 (1998).

10. D. K. Galloway *et al.*, *Astrophys. J. Suppl. Ser.* **179**, 360 (2008).

11. X. L. Tu *et al.*, *Phys. Rev. Lett.* **106**, 112501 (11 Mar. 2011).

12. C. Langer *et al.*, *Phys. Rev. Lett.* **113**, 032502 (3 July 2014).

13. O. Forstner *et al.*, *Phys. Rev. C* **64**, 045801 (4 Aug. 2001).

14. R. Cyburt *et al.*, Private Communication, (2016).

15. X. Tu *et al.*, *Nuc. Phys. A* **945**, 89 –94 (2016).

16. J. Tian *et al.*, *Phys. Rev. C* **87**, 014313 (1 Jan. 2013).

17. B. A. Brown *et al.*, *Phys. Rev. C* **65**, 045802 (4 Jan. 2002).

18. P. Van Isacker *et al.*, *Phys. Rev. Lett.* **74**, 4607–4610 (23 June 1995).

19. P. Van Isacker *et al.*, *Phys. Rev. Lett.* **82**, 2060–2063 (10 Mar. 1999).

20. A. Jokinen *et al.*, *Eur. Phys. J. A* **3**, 271–276 (1998).

21. Kankainen, A. *et al.*, *Eur. Phys. J. A* **25**, 129–130 (2005).

22. H. Fujita *et al.*, *Phys. Rev. C* **75**, 034310 (3 Mar. 2007).

23. M. Mukherjee *et al.*, *Eur. Phys. J. A* **35**, 1–29 (2008).

24. R. Wolf *et al.*, *Nucl. Instrum. Methods A* **686**, 82 –90 (2012).

25. S. Kreim *et al.*, *Nucl. Instrum. Methods B* **317**, 492 –500 (2013).

26. R. N. Wolf *et al.*, *Int. J. Mass Spectr.* **313**, 8–14 (2012).

27. F. Wienholtz *et al.*, *Nature* **498**, 346–349 (2013).

28. M. Rosenbusch *et al.*, *Phys. Rev. Lett.* **114**, 202501 (20 May 2015).

29. D. Atanasov *et al.*, *Phys. Rev. Lett.* **115**, 232501 (23 Dec. 2015).

30. M. König *et al.*, *Int. J. Mass Spectrom* **142**, 95 –116 (1995).

31. C. D. Nesaraja *et al.*, *Nuc. Data Sheets* **111**, 897 –1092 (2010).

32. R. Borcea *et al.*, *Nuc. Phys. A* **695**, 69 –81 (2001).

33. U. Köster *et al.*, *Nuc. Instrum. Methods B* **204**, 303 –313 (2003).

Appendix

DESCRIPTION OF THE PROPOSED EXPERIMENT
The experimental setup comprises: ISOLDE central beam line and ISOLTRAP setup. The ISOLTRAP setup has safety clearance, the memorandum document 1242456 ver.1 Safety clearance for the operation of the ISOLTRAP experiment by HSE Unit is released and can be found via the following link: https://edms.cern.ch/document/1242456/1.

Part of the	Availability	Design and manufacturing
ISOLTRAP setup	☒ Existing	☒ To be used without any modification

HAZARDS GENERATED BY THE EXPERIMENT (if using fixed installation:) Hazards named in the document relevant for the fixed ISOLTRAP installation.